British Journal of Pharmacology

DOI:10.1111/j.1476-5381.2011.01346.x
www.brjpharmacol.org

RESEARCH PAPER

The proton translocation domain of cellular vacuolar ATPase provides a target for the treatment of influenza A virus infections

Konstantin H Müller[1], Denis E Kainov[1]*, Karim El Bakkouri[2,3], Xavier Saelens[2,3], Jef K De Brabander[4,5], Christian Kittel[6], Elisabeth Samm[6] and Claude P Muller[1]

[1]*Institute of Immunology, Centre de Recherche Public-Santé/Laboratoire National de la Santé, Luxembourg, Luxembourg,* [2]*Department for Molecular Biomedical Research, VIB, Ghent, Belgium,* [3]*Department for Biomedical Molecular Biology, Ghent University, Ghent, Belgium,* [4]*Department of Biochemistry, University of Texas Southwestern Center at Dallas, Dallas, TX, USA,* [5]*Harold C. Simmons Comprehensive Cancer Center, University of Texas Southwestern Medical Center at Dallas, Dallas, TX, USA, and* [6]*Avir Green Hills Biotechnology AG, Vienna, Austria*

Correspondence
Claude P. Muller, Institute of Immunology, Centre de Recherche Public-Santé/ Laboratoire National de la Santé, L-1950 Luxembourg, Luxembourg. E-mail: Claude.Muller@LNS.ETAT.LU

*Present address: Institute for Molecular Medicine Finland (FIMM), University of Helsinki, FI-00014, Finland.

Keywords
v-ATPase; v-ATPase inhibitor; influenza A virus; pandemic H1N1; H5N1; concanamycin A; bafilomycin A1; archazolid B; salicylihalamide A derivatives; saliphenylhalamide

Received
24 March 2010
Revised
28 January 2011
Accepted
25 February 2011

BACKGROUND AND PURPOSE

Cellular vacuolar ATPases (v-ATPase) play an important role in endosomal acidification, a critical step in influenza A virus (IAV) host cell infection. We investigated the antiviral activity of the v-ATPase inhibitor saliphenylhalamide (SaliPhe) and compared it with several older v-ATPase inhibitors concanamycin A, bafilomycin A1, (BafA) and archazolid B targeting the subunit c of the V_0 sector.

EXPERIMENTAL APPROACH

An *in vitro* assay was devised to quantify the anti-influenza effect of v-ATPase inhibitors by measuring green fluorescent protein fluorescence of a reporter IAV. These data were combined with cytotoxicity testing to calculate selectivity indices. Data were validated by testing v-ATPase inhibitors against wild-type IAV *in vitro* and *in vivo* in mice.

KEY RESULTS

In vitro SaliPhe blocked the proliferation of pandemic and multidrug resistant viruses at concentrations up to 51-fold below its cytotoxic concentrations. At essentially non-toxic concentrations, SaliPhe protected 62.5% of mice against a lethal challenge of a mouse-adapted influenza strain, while BafA at cytotoxic concentrations showed essentially no protection against infection with IAV (SaliPhe vs. BafA $P < 0.001$).

CONCLUSIONS AND IMPLICATIONS

Our results show that a distinct binding site of the proton translocation domain of cellular v-ATPase can be selectively targeted by a new generation v-ATPase inhibitor with reduced toxicity to treat influenza virus infections, including multi-resistant strains. Treatment strategies against influenza that target host cellular proteins are expected to be more resistant to virus mutations than drugs blocking viral proteins.

Abbreviations

ArchB, archazolid B; BafA, bafilomycin A1; ConmyA, concanamycin A; H1N1 OR, H1N1 oseltamivir resistant; IAV, influenza A virus; MDCK, Madin–Darby canine kidney; MOI, multiplicity of infection; SaliA, salicylihalamide A; SaliPhe, saliphenylhalamide; SI, selectivity index; S-OIV, swine origin pandemic influenza virus; v-ATPase, vacuolar-ATPase; VGM, virus growth medium

Introduction

Influenza A viruses (IAVs) cause recurrent outbreaks in humans and animals, with serious consequences for public health and even the global economy. Rapid accumulation of mutations and reassortment of genomic segments between strains and subtypes enable new viruses to emerge by acquiring new properties including the development of resistance to antiviral drugs.

Current drugs against IAV are directed against two viral proteins. Adamantane-derived drugs like amantadine and rimantadine inhibit the activity of viral M2 protein. These drugs have been used for many years in community outbreaks, but current IAV strains have become resistant to these drugs and their use is no longer recommended. Today, the treatment of influenza infections largely depends on oseltamivir and zanamivir that inhibit viral neuraminidase. However, the rapid spread of resistance mutations in seasonal IAVs (Kiso *et al.*, 2004; Stephenson *et al.*, 2009) and their emergence in highly pathogenic avian influenza H5N1 (De Jong *et al.*, 2005) and in the recent pandemic A/H1N1 strain (Lackenby *et al.*, 2008) represent a major threat to public health. While antiviral drugs tend to select resistant strains, resistance has also developed independently of drug treatment (Lackenby *et al.*, 2008). Thus, there is an urgent need to develop antiviral strategies against influenza that are resistant to viral mutations. Targeting cellular proteins critical for viral replication could be a strategy to overcome IAV drug resistance.

Virus replication depends on a multitude of cellular functions and proteins. Several comprehensive studies have demonstrated that about 300 diverse cellular proteins are involved in IAV replication (Hao *et al.*, 2008; Brass *et al.*, 2009; König *et al.*, 2010; Karlas *et al.*, 2010). The regulatory interactions between cellular proteins and IAV have also been extensively studied (Shapira *et al.*, 2009). In comparison with many cellular proteins involved in viral replication, proteins involved in the early steps of viral life cycle are of particular interest. IAV enters the cell by endocytosis. Low pH in the late endosomes triggers fusion between viral and endosomal membranes mediated by haemagglutinin and the release of viral ribonucleoprotein particles into the cytosol. An inhibition of acidification can prevent IAV entry *in vitro* (Ott and Wunderli-Allenspach, 1994; Perez and Carrasco, 1994; Guinea and Carrasco, 1995; Ochiai *et al.*, 1995).

The vacuolar ATPases (v-ATPases) acidify the late endosome by pumping protons across the endosomal membrane. The v-ATPases are multisubunit molecular motors consisting of a cytosolic V_1 domain and a transmembrane V_0 domain. The V_1 domain consists of eight different proteins (Forgac, 1999), while the V_0 domain consists of six different proteins (Wang *et al.*, 2007). Various tissue-specific isoforms of certain subunits have been described (Sun-Wada *et al.*, 2003). The v-ATPases are found on membranes of different intracellular organelles as well as in cytoplasmic membranes, and are involved in a variety of cellular processes that require pH regulation including intracellular membrane transport, prohormone processing or transport of neurotransmitters (see Nishi and Forgac, 2002). Mutations in the v-ATPases can cause human diseases including renal acidosis (Smith *et al.*, 2000), male infertility (Pastor-Soler *et al.*, 2005) or osteopetrosis (Li *et al.*, 1999) and the v-ATPases are emerging as potential drug targets for the treatment of osteoporosis and cancer (Forgac, 1999; Lebreton *et al.*, 2008).

In the early antiviral studies against influenza and other viruses (e.g. Semliki Forest virus and vesicular stomatitis virus) (Perez and Carrasco, 1994), the plecomacrolide antibiotics bafilomycin A1 (BafA) and concanamycin A (ConmyA) were used to block v-ATPase activity (Figure 1). The plecomacrolides are potent inhibitors of v-ATPases and their mechanisms have been extensively studied. However, the ionophoric properties of plecomacrolides cause mitochondrial damage and cell apoptosis, and their toxicity is incompatible with their pharmacological use *in vivo* (Teplova *et al.*, 2007). Another group of v-ATPase inhibitors, the archazolides (Figure 1), are macrocyclic lactones with a thiazole side chain that is structurally distinct from the plecomacrolides, but share at least partially a common binding site on the V_0 subunit c (Huss *et al.*, 2005). Archazolid B (ArchB) was only slightly less toxic in A549 cells than BafA or ConmyA (Huss *et al.*, 2005) and because of their cytotoxicty, v-ATPase inhibitors have become an area of active research as anticancer drugs (Hinton *et al.*, 2009).

Benzolactone enamides, another group of v-ATPase inhibitors, were shown to inhibit mammalian v-ATPase at nM concentrations (Erickson *et al.*, 1997). Benzolactone enamides are specific for v-ATPases of mammalian cells and do not inhibit v-ATPases from yeast or other fungi (Boyd *et al.*, 2001). Salicylihalamides A (SaliA) and B were the first members of this group of compounds. SaliA acts irreversibly on the trans-membrane proton translocation domain via N-acyl iminium chemistry (Xie *et al.*, 2004). Saliphenylhalamide (SaliPhe, Figure 1), a phenyl derivative of SaliA, is more stable than SaliA. It has been shown that SaliPhe can discriminate between tumourigenic and non-tumourigenic mammary epithelial cells while SaliA harms both cell lines to a similar extent, indicating that SaliPhe has less cytotoxic off-target effects on non-tumour cells (Lebreton *et al.*, 2008).

Here, we have demonstrated that new and old generation v-ATPase inhibitors successfully inhibit viral entry *in vitro* of IAV strains of major public health concern, including oseltamivir resistant, pandemic and highly pathogenic avian strains, albeit with very different selectivity indices, indicating that the anti-IAV effect of v-ATPase inhibition is distinct from toxic side effects and that this can be exploited to treat IAV infections *in vivo*.

In contrast to BafA, SaliPhe protected against influenza infection in a mouse model. Our results show that a distinct binding site of the proton translocation domain of cellular v-ATPase can be targeted by a new generation v-ATPase inhibitor with reduced toxicity, in order to treat influenza virus infection including multiresistant strains. Treatment strategies against influenza that target cellular proteins would be more resistant to virus mutations than drugs blocking viral proteins.

Methods

Cells and viruses

Madin–Darby canine kidney (MDCK) cells were maintained in Dulbecco's modified Eagle's medium (Invitrogen, Merel-

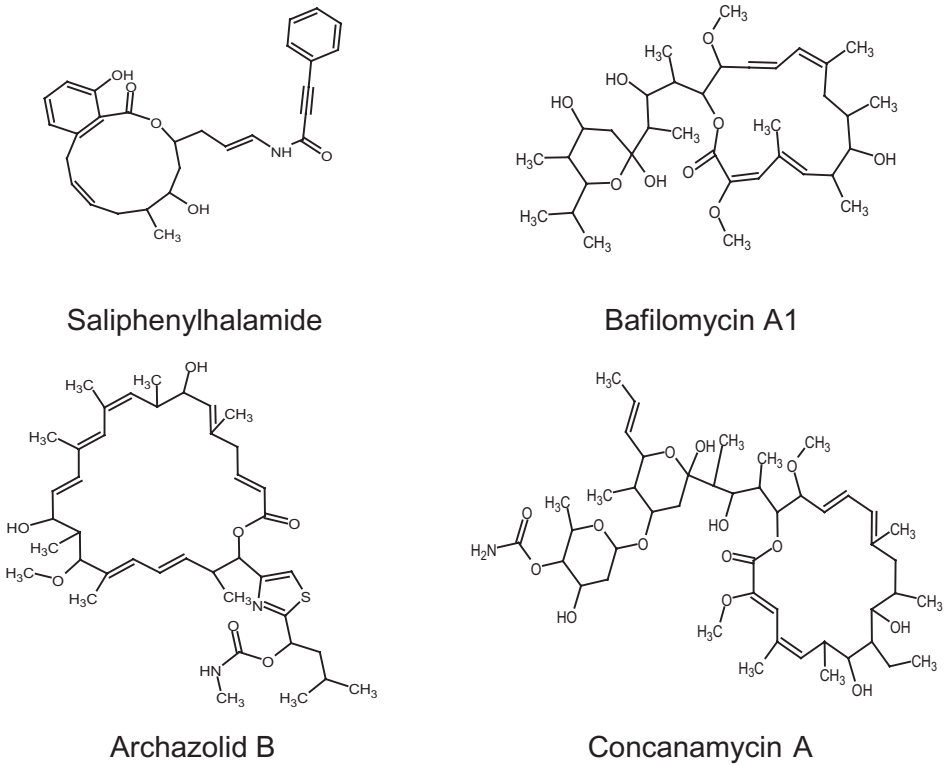

Figure 1

Structures of v-ATPase inhibitors. The benzolactone enamide saliphenylhalamide (a derivative of BafA and SaliA), the plecomacrolides, BaFA and ConmyA, and the macrolactone Arch B.

beke, Belgium) supplemented with 10% fetal bovine serum, 20 mM HEPES, 25 mg·mL^{-1} bovine serum albumin, 100 U·mL^{-1} penicillin and 100 U·mL^{-1} streptomycin. A549 cells were cultured in Eagle's minimal essential medium (EMEM) (Invitrogen) supplemented with 10% fetal bovine serum, 2 mM ultra-glutamine (Lonza, Verviers, Belgium), 100 U·mL^{-1} penicillin and 100 U·mL^{-1} streptomycin. For cultivation of virus or infection experiments, MDCK cells were overlaid with virus growth medium (VGM-MDCK), which represents serum-free MDCK culture medium containing 2 µg·mL^{-1} L-1-tosylamido-2-phenylethyl chloromethyl ketone-trypsin (TPCK-trypsin; Sigma-Aldrich, Bornem, Belgium). For infection experiments, A549 cells were overlaid with VGM-A549 consisting of serum-free A549 culture medium containing 1 µg·mL^{-1} TPCK-trypsin. All incubation steps involving cells were performed at 37°C and 5% CO_2.

The strains of IAV used in this study include swine origin H1N1 2009 (S-OIV) A/Hamburg/01/2009 (kindly provided by S. Becker, Marburg, Germany), A/Luxembourg/572/2008 (H1N1) resistant to oseltamivir (Gerloff *et al.*, 2009), A/Chicken/Nigeria/BA211/2006 (H5N1) (Ducatez *et al.*, 2007) and PR8-NS116-GFP virus (H1N1). PR8-NS116-GFP virus appeared as a spontaneous frame shift/deletion mutant during a rescue experiment as described previously (Kittel *et al.*, 2004). The fusion protein expressed by the chimeric NS segment consists of the N-terminal 104 aa of NS1 followed by 12 aa derived from the second NS frame and the green fluorescent protein (GFP) open reading frame. All viruses were titred both on MDCK and A549 cells to allow an identical multiplicity of infection (MOI) for both cell lines.

In vitro cytotoxicity assay

A 96-well plate was seeded with 3x10^3 cells per well in 99 µL cell culture medium. The v-ATPase inhibitors were dissolved in DMSO and 1 µL of 11 steps of a twofold serial dilution of eight replicates was added to a well. The final DMSO concentration was 1% in all wells. Controls included wells with 1% DMSO or medium. After 5 days of incubation, 50 µL of freshly prepared XTT reagent (Roche, Mannheim, Germany) was added to the wells and the plate was incubated for 2 h at 37°C. The plate was read at 450 and 650 nm on a SpectraMax plus 384 (Molecular Devices, Berkshire, UK).

Anti-IAV efficacy assay

The 96-well plates containing 7 x 10^4 adherent MDCK or A549 cells per well were washed three times with 200 µL of serum-free EMEM and overlaid with 99 µL VGM-MDCK or VGM-A549 containing IAV corresponding to a MOI of 0.03. The v-ATPase inhibitors were dissolved in DMSO and stocks were kept at –80°C. From these stocks, twofold serial dilutions were prepared in DMSO, 1 µL of each dilution was added to a well containing cells and virus. Dilutions were tested as duplicates or triplicates. Experiments employing NS1-GFP fusion IAV were performed in µClear bottom (black) plates (Greiner, Frickenhausen, Germany) and read after 24 h of incubation

on a Tecan Genios plus Reader (Tecan Group, Salzburg, Austria) using 485 nm excitation and 535 nm emission filters for GFP fluorescence. Representative images were taken on a Leitz DM IL microscope with separate mercury lamp and a Leica DFC480 camera (Wetzlar, Germany).

Unmodified wild-type (wt) IAVs were tested as follows: After 24 h of incubation, supernatant was transferred to a second plate; the attached cells in each well were lysed (150 µL lysis solution), recombined with 50 µL of supernatant and extracted with the MagMax total RNA kit (Ambion, Lennik, Belgium) on a KingFisher 96 instrument (Thermo Fisher Scientific, Breda, the Netherlands). The extracted total RNA was reverse transcribed using dT_{20} primers (Eurogentec, Seraing, Belgium) and SuperScript III (Invitrogen) according to the manufacturer's instructions and cDNA was quantified for IAV matrix gene (primers and probes by Ward *et al.*, 2004) and for canine β-actin (primers by Mak *et al.*, 2006).

β-Actin-specific RT-qPCRs was performed to normalize for the total amount of extracted RNA and to monitor cell survival within assays. Virus proliferation was expressed as percent of the difference between cultures with virus and the lowest (or zero) drug concentration, and cultures without virus. To control for background noise resulting from surviving virus of the initial inoculate, an identical amount of virus was incubated in cell-free medium and tested by qPCR.

Mouse experiments

All experiments were carried out under BSL-2 conditions and in compliance with animal welfare regulations of Luxembourg and Belgium including local guidelines of the VIB Department for Molecular Biomedical Research, University of Ghent and the Laboratoire National de Santé/CRP-Santé. Specific pathogen-free female 6- to 7-week-old BALB/c mice (Charles River Laboratories, Calco Lecco, Italy) were used throughout the study.

The animals were housed in a temperature-controlled environment with 12 h light/dark cycles, and received food and water *ad libitum*. For the *in vivo* efficacy studies, mice were inoculated intranasally with 50 µL PBS with or without (mock infection) four mouse LD_{50} of mouse-adapted A/PR/8/34 strain. Body temperature was measured with a rectal probe, and body weight was monitored daily for either 14 days or until a 30% loss of body weight was observed, at which point mice were killed, according to national regulations. Mice were treated or mock-treated with a first dose of v-ATPase inhibitor 4 h before infection followed by i.p. injections every 8 h until day 9 post-infection. BafA was dosed at 350 $ng \cdot kg^{-1}$ in 200 µL PBS; an equal volume of PBS only was injected in the mock treatment group. SaliPhe was given at a dose of 7 $mg \cdot kg^{-1}$ resuspended in 200 µL Lipovenös 20% (Fresenius Kabi, Bad Homburg, Germany) three times daily; the mock treatment group received an equal volume of Lipovenös only. The dosing of SaliPhe was based on previous toxicity studies in mice where first signs of toxicity (neurotoxicicity) were observed above 7 $mg \cdot kg^{-1}$ (J. De Brabander, unpubl. results). Also, mock-infected groups received the same treatment with v-ATPase inhibitor. An additional group of mice that received no injections at all was included for comparison. Mice surviving until 15 days post-infection were euthanized by cervical dislocation, and lungs, spleens and livers were removed and preserved in neutral-buffered 10% formalin for histology.

Virus titration of lung tissues

For virus titration of the lungs, three mice per treatment group were inoculated intranasally with one mouse LD_{50} in 100 µL PBS of mouse-adapted A/PR/8/34 strain and killed 4 days post-infection to collect the lungs. Lung homogenates were prepared in 1.5 mL of PBS by using a microhomogeniser. The homogenate was cleared by centrifugation at 13 800× *g* for 15 min at 4°C. The extracts were transferred to centrifuge tubes and cell debris was pelleted for 5 min at 400 g and 4°C. The cleared lung extracts were stored at –80°C. Titres of infectious virus were determined in triplicate by titration on MDCK cells. Monolayers were infected for 1 h with 50 µL of serial 1:10 dilutions of the lung homogenates in a 96-well plate in serum-free Dulbecco's modified Eagle's medium (Invitrogen) supplemented with penicillin and streptomycin. Following inoculation, the supernatant was replaced by medium containing 2 $\mu g \cdot mL^{-1}$ trypsin. Endpoint virus titres were determined after 4 days, as described by Reed and Muench (1938), by interpolating the dilution that infected 50% of the wells, as assayed by haemagglutination of chicken red blood cells.

Histopathology

Formalin-fixed lung samples were embedded in paraffin. Serial 4 µm sections were double stained with haematoxylin and the mouse monoclonal anti-IAV matrix protein 2 antibody (14C2, Santa Cruz Biotechnology, Santa Cruz, CA, USA) and Dako Animal Research Kit on a Dako Autostainer Plus instrument. Representative images were taken on a Zeiss Axio Observer Z1 with a Zeiss AxioCam HRc color camera (Zaventem, Belgium).

Data analysis

Fluorescence data obtained in the GFP-based anti-IAV efficacy assay were fitted to a Hill curve with SigmaStat 9.0 software (SPSS Inc., Chicago, IL, USA) and EC_{50} values were calculated. The same fit was applied to c_t values obtained from qPCRs for viral matrix gene detection. Statistical significance tests were performed with Students *t*-test; $P < 0.05$ was considered significant.

Survival data of the mouse experiments were analysed with SigmaStat 9.0 using Gehan–Breslow Test.

Materials

ArchB was a kind gift of Dirk Trauner (Munich); ConmyA and BafA were purchased from Sigma-Aldrich and Fluka (Bornem, Belgium); SaliPhe was synthesized by Jef De Brabander's group (Lebreton *et al.*, 2008) All v-ATPase inhibitors used in this report target the lysosomal H^+ transporting ATPase (*ATP6*) (Smith *et al.*, 2003).

Results

Drug cytotoxicity

In order to determine the *in vitro* cytotoxicity of the v-ATPase inhibitors (Figure 1), increasing concentrations of the com-

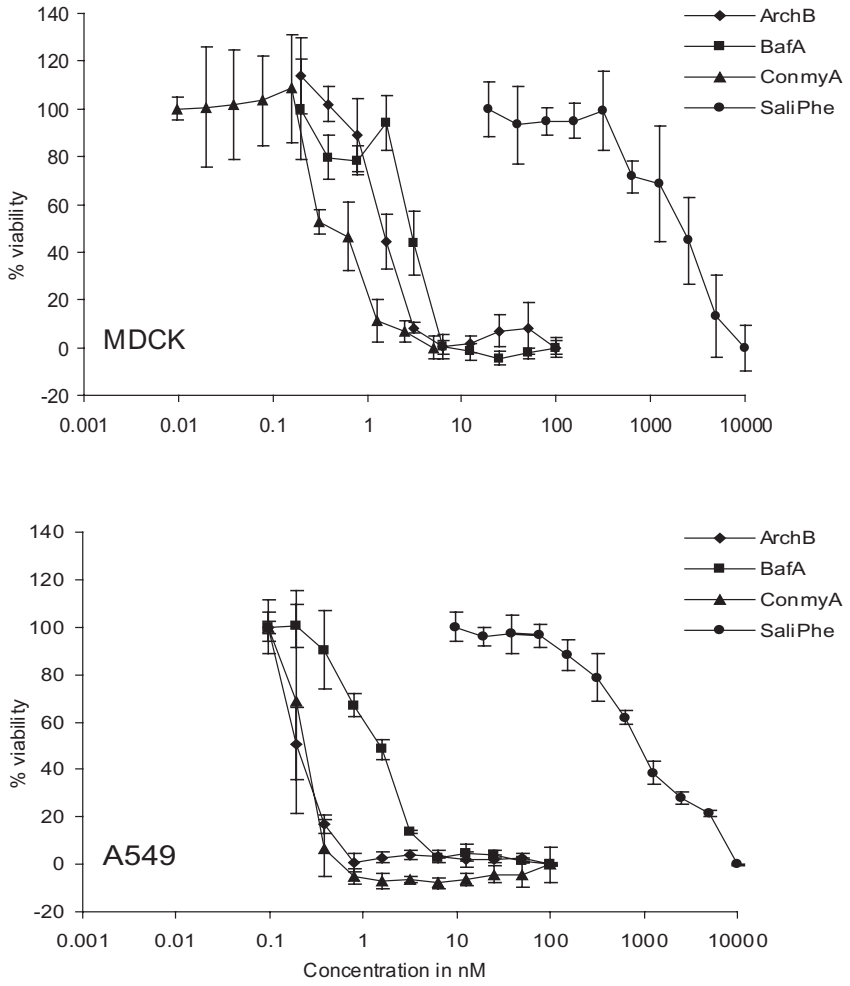

Figure 2

Cytotoxicity of v-ATPase inhibitors. Percent viability of MDCK and A549 cells was determined in the presence of increasing concentrations of v-ATPase inhibitors on the basis of eight replicates of XTT tests normalized to the absorbance at 450 nm of a drug-free culture containing 1% DMSO. Medium only corresponds to 0% viability. All measurements were corrected with a reference measurement at 650 nm. IC_{50} was deduced by fitting the obtained absorbance/concentration pairs to a dose-response curve.

pounds were added to MDCK or A549 cells. After 5 days, the half maximal concentrations inhibiting cell growth (IC_{50}) were determined using a standard XTT assay. Interestingly, in both MDCK and A549 cells (Figure 2), SaliPhe had the lowest cytotoxicity (IC_{50} of 1.74 ± 0.2 μM and 1 ± 0.19 μM), while the IC_{50} of the other established v-ATPase inhibitors ArchB (1.4 ± 0.1 nM and 0.16 ± 0.02 nM), BafA (2.9 ± 0.1 nM and 1.3 ± 0.2 nM) and ConmyA (0.56 ± 0.09 nM and 0.2 ± 0.02 nM) were in the low nM range or below.

In vitro antiviral activity of v-ATPase inhibitors against GFP – expressing IAV

In order to test candidate drugs for anti-IAV activity on A549 and MDCK cells, an *in vitro* assay based on a recombinant GFP-expressing IAV (PR8-NS116-GFP) was established. GFP fluorescence was used as a convenient surrogate read-out to quantify viral infection. The virus was titrated from 0.1 to 0.002 MOI to determine the optimal virus concentration (Figure 3). An MOI of 0.025 to 0.05 gave an optimal fluorescence read-out after 24 h. An MOI of 0.03 was used as a standard dose in all subsequent *in vitro* antiviral tests.

To test the antiviral activity of v-ATPase inhibitors, increasing concentrations of the compounds were added to cells infected with 0.03 MOI PR8-NS116-GFP IAV. GFP fluorescence intensity showed a dose-dependent reduction with increasing amounts of v-ATPase inhibitors. Figure 4 shows for each compound the anti-IAV dose-response curve in MDCK cells in comparison with the cytotoxic effect of the drugs (from Figure 2). The two dose-response curves of ArchB, BafA and SaliPhe did not overlap completely, indicating that these v-ATPase inhibitors inhibited viral growth at concentrations that were not cytotoxic *in vitro*. This was also reflected in the selectivity index (SI) (IC_{50}/EC_{50}) which was between 8 and 51 for these compounds (Figure 4). Thus, the reduced GFP fluorescence was the result of reduced viral proliferation and not of drug cytotoxicity. The ratio between desired anti-IAV activ-

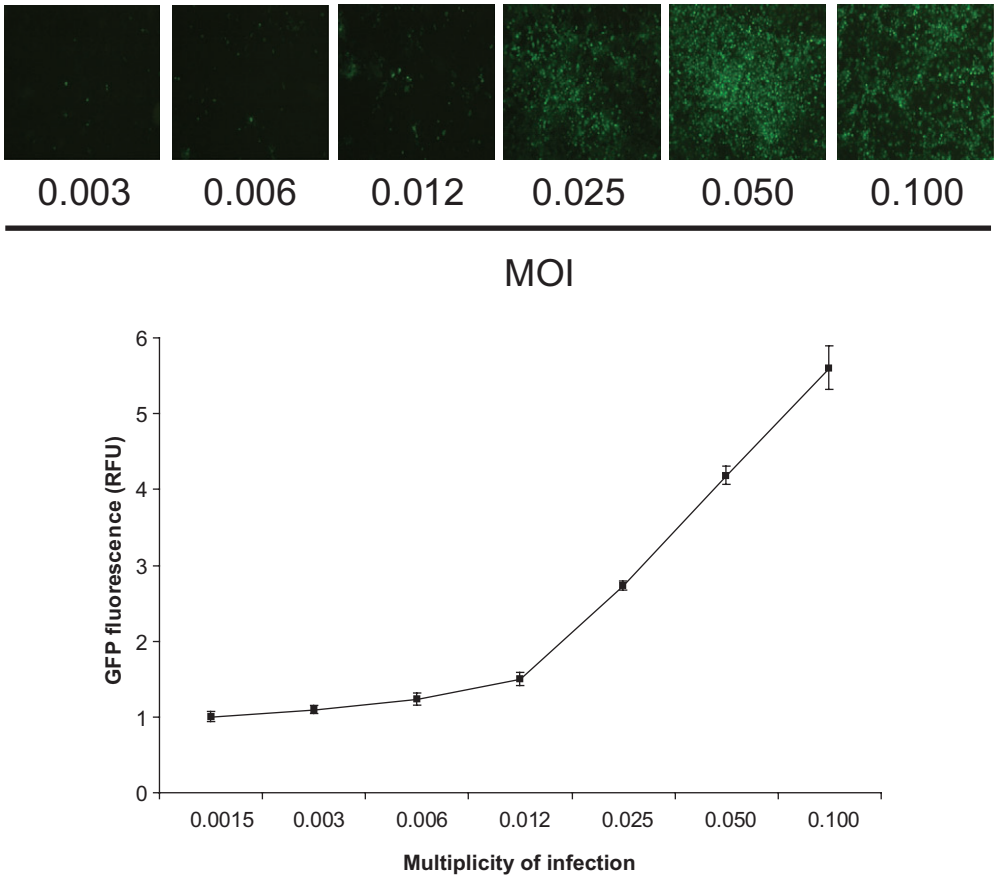

Figure 3

Titration of the fluorescence signal of a culture of GFP-expressing IAV. Fluorescence micrographs and fluorescence measurements of MDCK cells 24 h after infection with increasing multiplicity of infection (MOI) of PR8-NS116-GFP virus. Fluorescence is expressed in relative fluorescence units (RFU). Representative experiment repeated multiple times.

ity and toxic side effects was especially advantageous for SaliPhe and to a lesser extent for BafA.

This antiviral effect of v-ATPase inhibitors was also confirmed in the human epithelial lung cell line A549 (Figure 4) where the SI ranged from 3 to 13. All v-ATPase inhibitors completely inhibited viral growth, but SaliPhe had the highest SI values (SI 13) followed by BafA (SI 7) (Figure 4).

From the cytotoxicity dose-response curves, in Figure 2 the IC_5 concentrations corresponding to 95% cell survival were determined. A direct comparison of the anti-IAV activity of v-ATPase inhibitors at IC_5 concentrations of all drugs (350 nM SaliPhe; 0.6 nM ArchB; 0.6 nM BafA; 0.1 nM ConmyA) on PR8-NS116-GFP (MOI 0.05) showed that all v-ATPase inhibitors except ConmyA can inhibit viral proliferation at subtoxic concentrations compared with DMSO controls (data not shown).

In vitro antiviral activity of v-ATPase inhibitors against wt IAV isolates

NS1 is an important virulence factor of IAV and its partial replacement with GFP leads to reduced virus growth (Garcia-Sastre *et al.*, 1998; Kittel *et al.*, 2004) especially in interferon-competent cells such as MDCK or A549. Therefore, antiviral activity of the compounds was also tested against unmodified wild-type (wt) IAV, including pandemic S-OIV, highly pathogenic avian influenza H5N1 virus (A/Chicken/Nigeria/BA211/2006) and an oseltamivir-resistant seasonal H1N1 strain (A/Luxembourg/572/2008). MDCK cells were infected with 0.03 MOI of these wt viruses and serial dilutions of v-ATPase inhibitors were added. Drug-free DMSO-diluent served as a negative drug control. Viral replication was monitored by standard matrix gene qPCR after total RNA extraction and reverse transcription (Figure 5).

The c_t values of the dilution series of each compound were fitted to a dose-response curve to obtain EC_{50} values. These were again compared with the IC_{50} values of Figure 2 for each cell line and the SI was calculated. For the oseltamivir-resistant H1N1 isolate, the SI ranged from 0.5 for ConmyA to 61 for SaliPhe (Figure 5). Thus, SaliPhe was at least as active against a seasonal H1N1 virus as against the PR8-NS116-GFP IAV. SaliPhe proved to be also highly effective, against the pandemic H1N1 isolate A/Hamburg/01/2009 (SI of 48). However, SaliPhe was six times less active against the HPAI H5N1 virus (SI value of 8.5) than against the PR8-NS116-GFP. In contrast, the cytotoxicity and drug response curves of ConmyA and ArchB largely overlap and their SIs were below 3. BafA was intermediate with SI values up to 8. Thus,

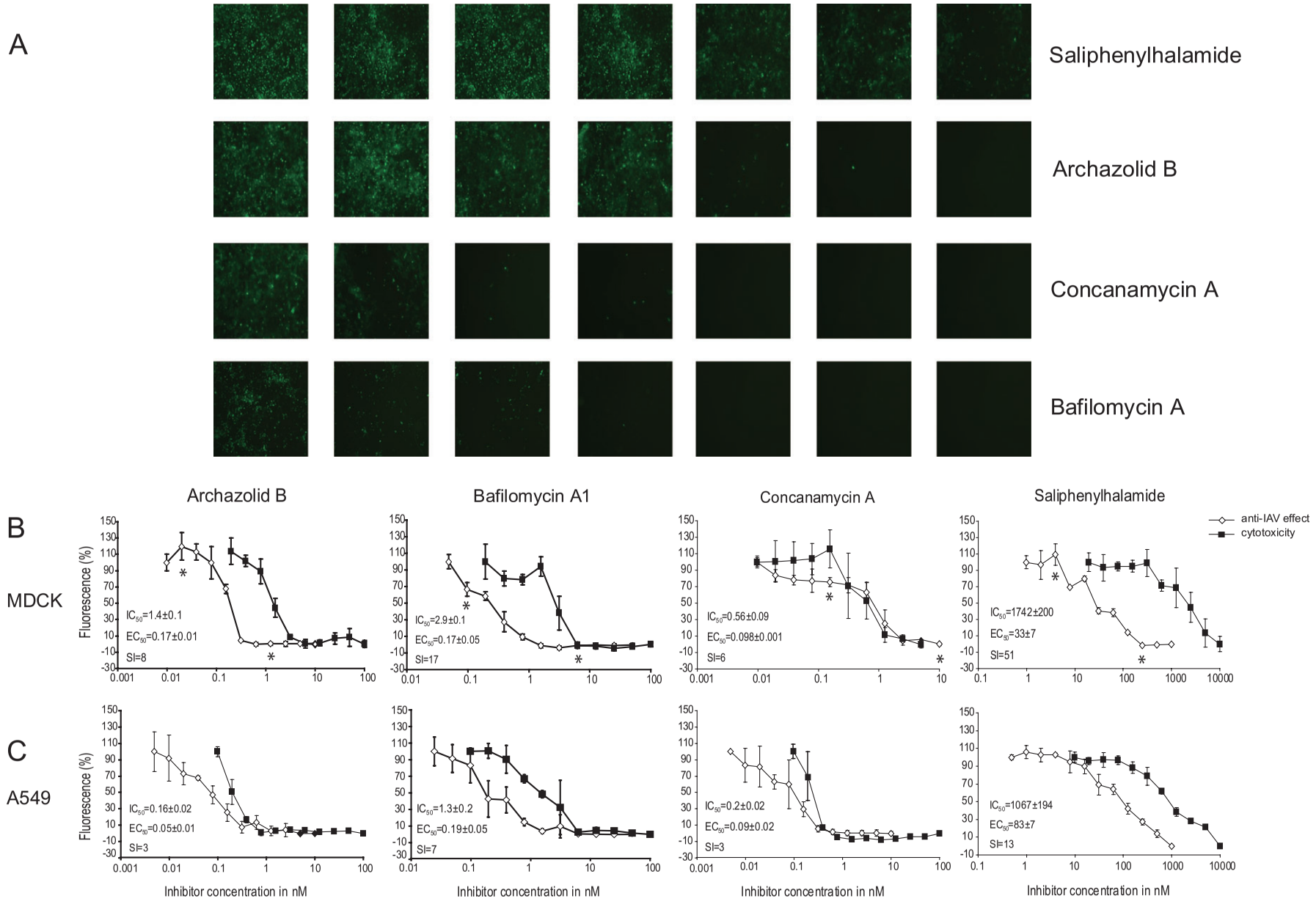

Figure 4

Antiviral efficacy of v-ATPase inhibitors against the GFP-expressing IAV. (A) Representative fluorescence micrographs of MDCK cell cultures infected with a MOI of 0.03 of PR8-NS116-GFP incubated with increasing concentrations of v-ATPase inhibitors. Drug concentrations between ** in panel B are shown. (B,C) Anti-IAV activity of v-ATPase inhibitors against PR8-NS1116-GFP virus in MDCK (B) and A549 cells (C). The curves represent the percent fluorescence of cultures with the lowest concentration of drug and were used to calculate the EC_{50}. Each data point represents the mean of a triplicate culture of a representative experiment repeated at least twice. The cytotoxicity of the inhibitors (from Figure 2) is shown for comparison. The SI was calculated as the ratio of IC_{50}/EC_{50}.

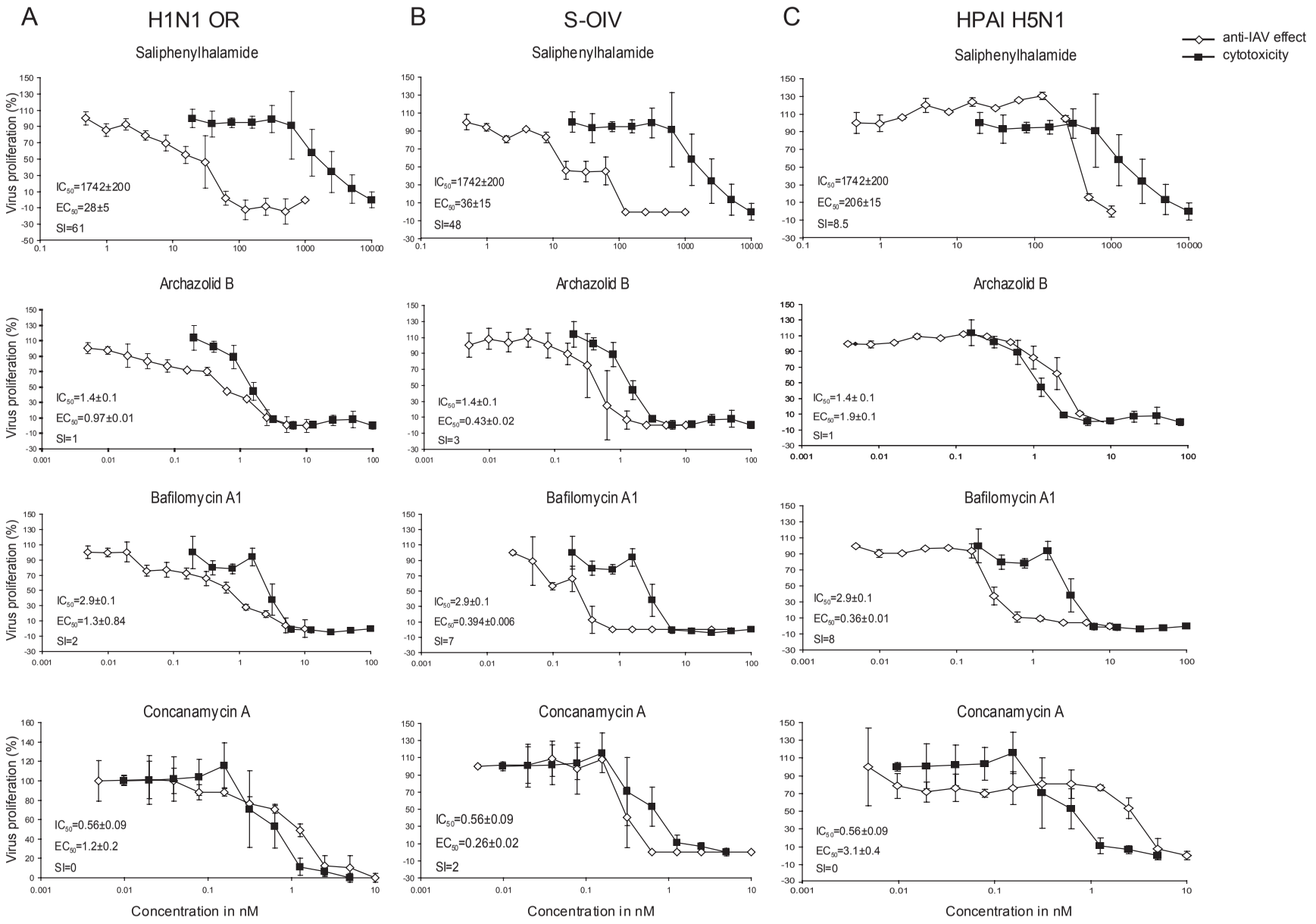

Figure 5

Antiviral efficacy of v-ATPase inhibitors against wild-type (wt) viruses. Antiviral effect of the four v-ATPase inhibitors against three wt IAV isolates: oseltamivir-resistant seasonal H1N1 (H1N1 OR), swine origin pandemic influenza virus (S-OIV) and highly pathogenic (HPAI) H5N1 on MDCK cells. The virus was quantified by quantitative PCR (c_t values) and was expressed in percent of Δc_t values of the lowest drug concentration and virus-free cultures. Raw data were fitted to Hill curves to calculate the EC_{50} shown in the inserts. Essentially, the same results are obtained if calculated in percent of drug-free cultures containing DMSO only. Each data point represents a cell culture triplicate of a representative experiment that was repeated at least twice. The cytotoxicity of the inhibitors (from Figure 2) is shown for comparison (closed squares). The SI was calculated as the ratio IC_{50}/EC_{50}. Standard deviation (S.D.) is occasionally smaller than symbols.

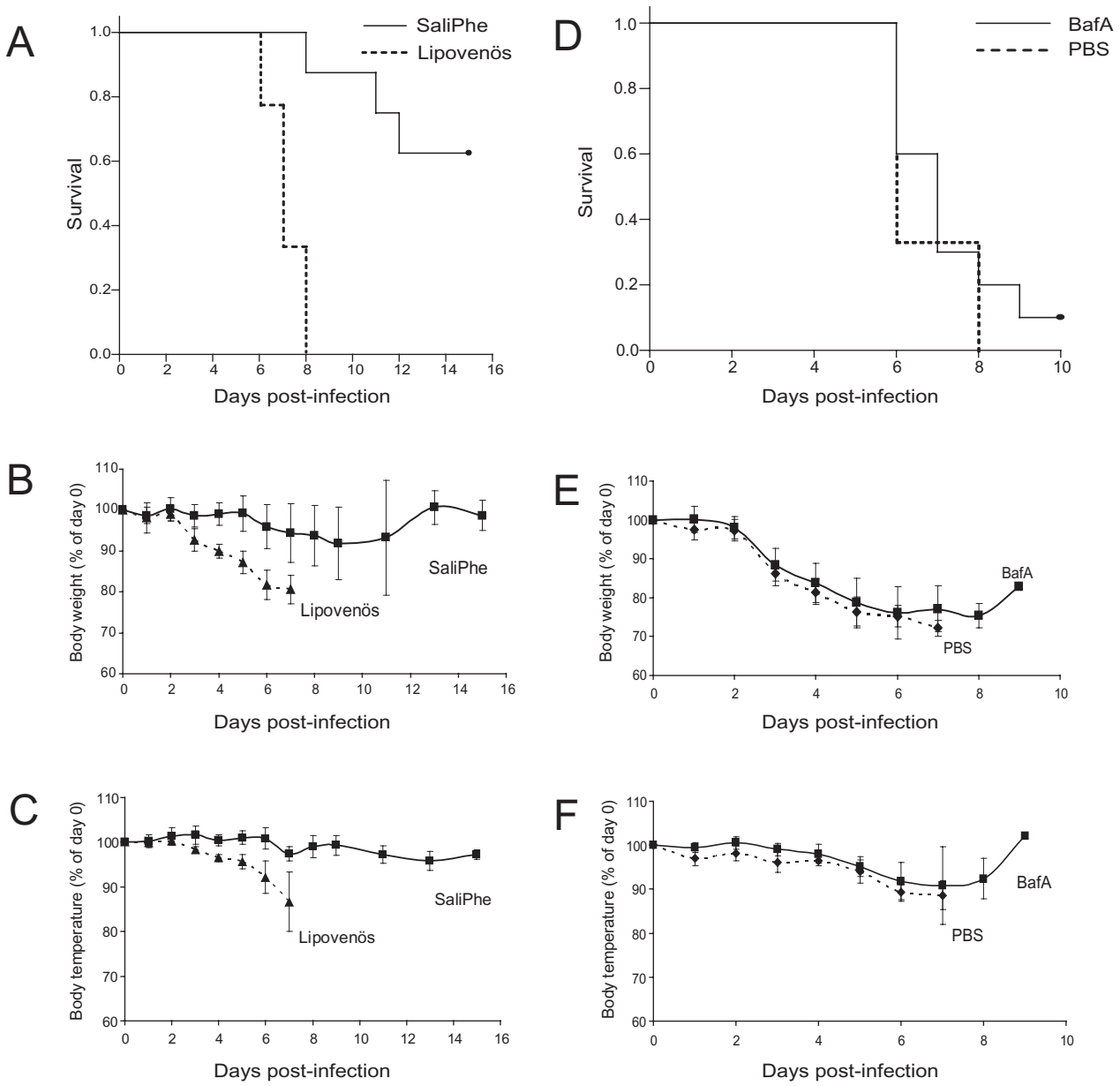

Figure 6

SaliPhe protects mice against influenza virus. (A,D) Kaplan–Meier survival curves of mice challenged with four mouse LD_{50} of mouse-adapted PR8 treated with SaliPhe (eight mice) or with Lipovenös only (nine mice) (A) and treated with BafA (10 mice) or PBS only (nine mice) (D). Body weight (B,E) and body temperature (C,F) of the same SaliPhe group (B,C) and BafA group (E,F) expressed in percent of day 0.

v-ATPase inhibitors also show antiviral activity against wt influenza viruses and in all cases SaliPhe was the most effective drug. These findings also confirm the results of the PR8-NS116-GFP-based assay.

In vivo anti-IAV activity of SaliPhe and BafA

The antiviral activities of the two v-ATPase inhibitors with the best SI *in vitro*, SaliPhe and BafA, were further tested in a standard mouse model of influenza infection. Mice were challenged with four mouse LD_{50} of mouse-adapted A/PR/8/34 virus and treated three times daily with injections of 7 mg·kg^{-1} SaliPhe in Lipovenös or 350 ng·kg^{-1} BafA in PBS every 8 h. The first dose of v-ATPase inhibitor was given 4 h before infection. Kaplan–Meier survival curves (Figure 6A,D) showed that all mock-treated animals (Lipovenös or PBS) died (or were killed when they reached the maximal permitted weight loss) as a result of the viral infection, whereas 62.5 % of the SaliPhe-treated animals survived and recovered from IAV infection until the end of the experiment 15 days post-infection although SaliPhe treatment was discontinued on day 9 post-infection. This difference in survival between SaliPhe and mock treatment was highly significant ($P < 0.001$ for SaliPhe vs. only Lipovenös; Gehan–Breslow test). In the

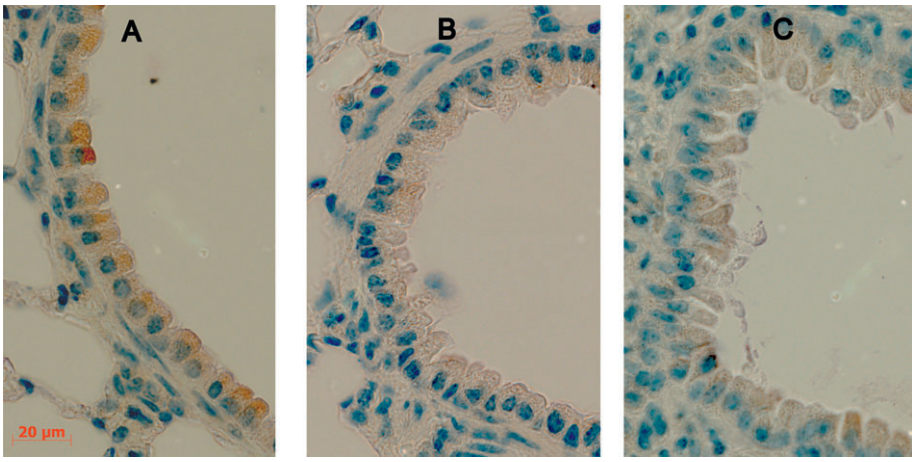

Figure 7

SaliPhe clears IAV from the lung. Immunohistochemistry of IAV infection in mouse lungs using an anti-matrix protein antibody and the Dako Animal Research Kit for visualization. (A) Positive control of an infected untreated mouse, all bronchiolar epithelial cells are stained; (B) negative control of mock-infected mouse. (C) Representative image of a lung of a mouse that was treated with SaliPhe and had cleared the virus by day 15 post-infection.

BafA treated group, only one mouse survived (BafA vs. PBS group: $P = 0.350$; BafA vs. SaliPhe: $P < 0.001$) (Figure 6A,D).

The weight of the animals was monitored as a measure of disease progression (Figure 6B,E). SaliPhe-treated mice showed only a limited average weight loss of less than 10% during the infection, which had fully recovered by 11 days post-infection. In contrast, Lipovenös mock-treated mice experienced a rapid and severe weight loss before dying (or being killed). Mice receiving BafA or PBS injections showed a steady loss of weight, and there was no difference up to day 7 post-infection between both groups. On later days, the weight gain was due to a single mouse recovering from the infection (Figure 6E).

SaliPhe-treated mice maintained their body temperature while Lipovenös mock-treated mice showed a drop of 13.4% (up to 6.5°C in one mouse) of their initial temperature, confirming disease progression (Figure 6C). No significant difference can be seen between body temperature curves obtained from BafA or PBS-treated mice except for the recovery of one surviving mouse on day 9 post-infection (Figure 6F).

Interestingly, the survival outcome of this experiment could not be improved by increasing the amount of SaliPhe per injection, extending the duration of treatment or decreasing the dose of virus used for infection, but in all cases survival in the SaliPhe-treated group was significantly better than mock-treated control groups (data not shown).

Virus replication in the lung

Four days post-infection, three mice of each treatment group were killed to determine viral titres in the lung. Although the SaliPhe-treated mice had over 90% reduction in virus titre, relative to that in the Lipovenös-treated mice with only three mice tested, this effect was not statistically significant ($P = 0.176$). Lungs of BafA and mock-treated mice showed very similar viral titres in both groups.

Viral infiltration of lungs was also examined by immunohistochemistry using an anti-matrix antibody. Virus-infected and mock-treated mice showed massive viral infections of the bronchiolar epithelial cells at the time of death (or being killed) (Figure 7A). No staining was visible in mock-infected negative control mice (Figure 7B). In the surviving SaliPhe-treated mice (killed on day 15), the virus was essentially cleared (Figure 7C).

In vivo toxicity

To control for toxic side effects of v-ATPase inhibitor treatment, a mock-infected group received a complete 10-day treatment course (injections every 8 h) of either BafA or SaliPhe. SaliPhe-treated mice showed ruffled fur during the first 3 days of treatment compared with the untreated group, but no fatalities occurred. Body weight of SaliPhe-treated and Lipovenös mock-treated mice slightly increased to the same extent in both groups, probably as a result of the nutritional effect of Lipovenös (Figure 8A). Body weight in the BafA-treated versus PBS-treated group remained constant (Figure 8B). There was virtually no change in body temperature in any of these mock-infected groups (Figure 8B,E).

To further investigate toxic effects, all mice were dissected at the end of the observation period (9 days post-mock infection), and spleen, liver and lungs were examined and weighed. There was no difference in the weight of spleens and livers between the SaliPhe-treated groups and the mock-treated groups (Figure 8C). There were also no obvious signs of toxicity in the histological preparations of the organs of these mice (data not shown). In contrast, BafA-treated mice showed a reduced weight of the spleens ($P = 0.1$) and livers ($P = 0.05$) in comparison with PBS-treated mice (Figure 8F), indicating potential toxic side effects on these organs, and non-specific histopathological signs of toxicity.

Discussion and conclusions

To test anti-IAV activity of old and new v-ATPase inhibitors, a novel assay was developed that allowed the monitoring of

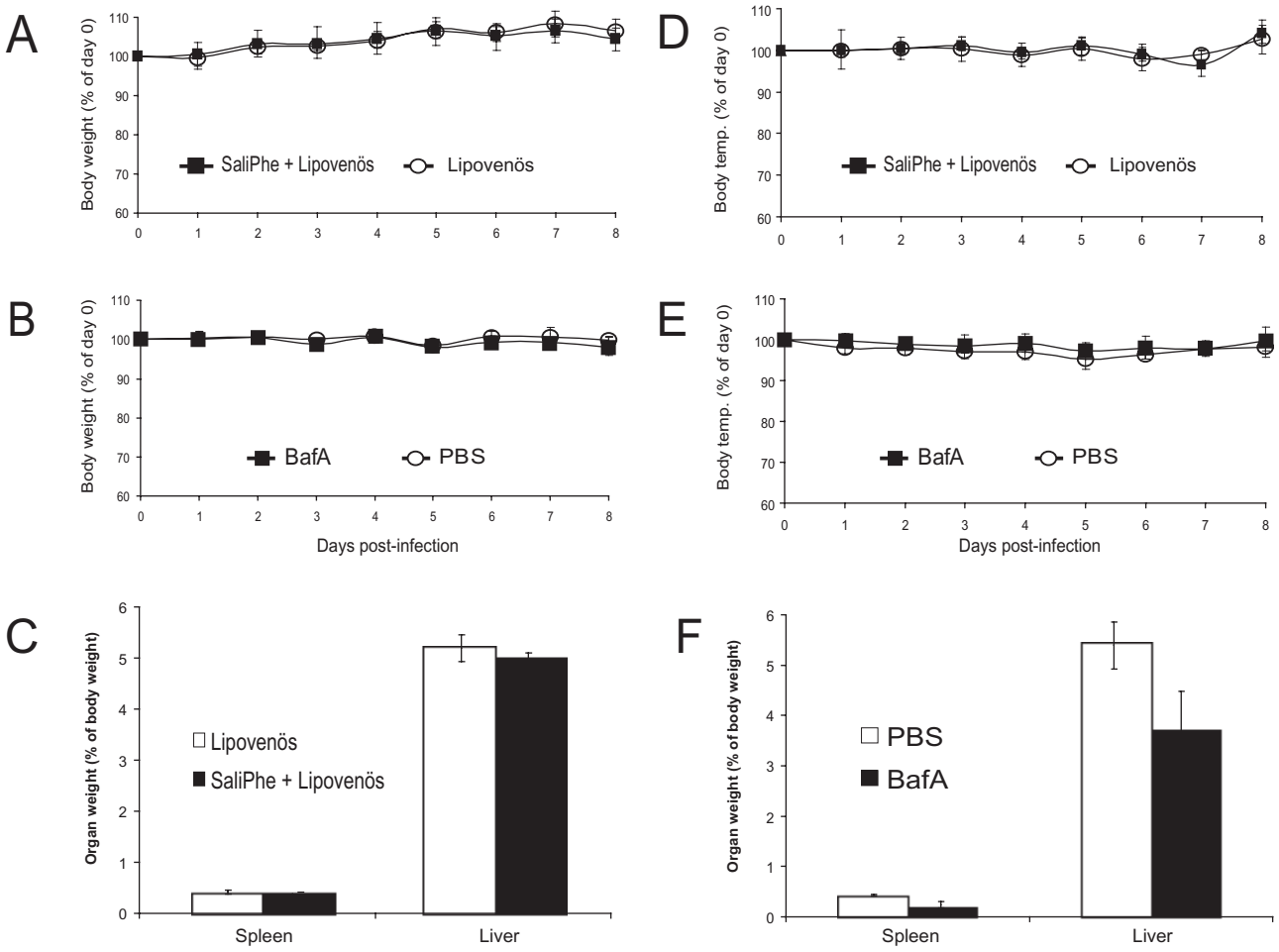

Figure 8

In vivo toxicity of SaliPhe and BafA. Body weight (A,B), body temperature (D,E) and organ weights (C,F) of mock infected mice, treated with standard protocol of SaliPhe (nine animals) (A,D) or BafA (12 animals) (B,E) in comparison with diluent treated mice (Lipovenös, nine mice; or PBS, 12 mice). Body weights and temperature are expressed in percent of day 0. (C,F) Weights of spleens and livers expressed in percent of body weight. Standard deviation (S.D.) is occasionally smaller than symbols.

viral growth by measuring the fluorescence of intracellular GFP encoded by a viral GFP-NS1 fusion gene. The strength of the assay is that the PR8-NS116-GFP IAV undergoes a complete natural replication cycle *in vitro*, involving most of the interactions between host cell proteins and wt virus proteins except full-size NS1. The assay can be readily adapted to high-throughput screening of compound libraries to detect anti-IAV activity.

In *in vitro* experiments, SaliPhe, a new generation v-ATPase inhibitor, was active against wt IAV isolates that are of major public health concern. While the cytotoxicity of this v-ATPase inhibitor was in the μM range, antiviral activity ranged from 28 nM to 206 nM. The other v-ATPase inhibitors tested were also active against influenza viruses but they were cytotoxic in the nanomolar and subnanomolar range.

On the basis of *in vitro* experiments with modified and unmodified IAVs, the two compounds SaliPhe and BafA were selected to compare their antiviral activity in mice. These experiments showed for the first time that certain v-ATPase inhibitors could be used to successfully treat IAV infections *in vivo*. This is also one of the first reports of a successful treatment of influenza *in vivo* by targeting a cellular protein critical for viral replication. Mazur *et al*. (2007) have previously shown that blocking NF-κB by intratracheal instillation of acetylsalicylic acid also partially protected mice against an H7N7 strain.

At a concentration which showed essentially no toxic effect, about 2/3 of the mice were protected by SaliPhe against a lethal infection with a mouse-adapted influenza virus. In contrast, BafA showed essentially no protection at toxic concentrations that resulted in spleen and liver damage. Incomplete protection in the SaliPhe treatment group can be partially attributed to dose limitations because of toxicity, but also to limitation of the treatment protocol in mice. After intravenous bolus injection in PEG/PBS (60:40), SaliPhe had a biological half-life of 40 min (J. De Brabander, unpubl. obs.). Although i.p. injection in a lipid emulsion may extend the half-life of drugs (Wang *et al*., 2005), the continuous infusion of subtoxic doses would probably give a better result, if the solubility problems can be solved. The short half-life of

Table 1

v-ATPase subunits identified by siRNA screens as host factors for virus replication

Virus	Cell line	v-ATPase genes	Reference
Influenza	A549	ATP6AP1, ATP6V0B, ATP6V0C, ATP6V0D1, ATP6V1A, ATP6V1B2	König *et al.*, 2010
Influenza	A549/293T	ATP6AP1, ATP6AP2, ATP6V0C, ATP6V1A, ATP6V0D1, ATP6V1B2,	Karlas *et al.*, 2010
Influenza	D-Mel2	ATP6V0D1, ATP6V0C	Hao *et al.*, 2008
Influenza	A549	A549ATP6AP1, ATP6V0B, ATP6V1G1	Brass *et al.*, 2009
Dengue	D-Mel2	ATP6AP1, ATP6AP2, ATP6V0B, ATP6V0C, ATP6V0D1, ATP6V1B2	Sessions *et al.*, 2009
WNV	HeLa	ATP6AP1, ATP6V0B, ATP6V0C, ATP6V0D1, ATP6V1A, ATP6V1B2	Krishnan *et al.*, 2008
HIV	293T	ATP6V0C	König *et al.*, 2008

SaliPhe may be compatible with inhalation as dry powder or as aerosol, delivering the drug to the lung epithelial cells which are both the portal of entrance and the main target organ of IAV. It is possible that intratracheal instead of parenteral delivery of SaliPhe can improve its protective potential *in vivo*.

The two macrolide antibiotics ConmyA and BafA were identified as v-ATPase inhibitors. However, the toxicity in animals precluded their use as antivirals and the approach was essentially given up in the 1990s. Because of their toxicity, research on v-ATPase inhibitors has concentrated on their cytotoxicity effects as anti-cancer drugs. Here we show that SaliPhe, a new generation v-ATPase inhibitor, is much less toxic than the earlier compounds, without compromising its activity. Their differences in relative antiviral and toxic activity suggest differences in their mode of action. BafA, ArchB and ConmyA interact with subunit c of the V_0 domain as seen in the decreased sensitivity to BafA in mutational studies with this subunit (Bowman and Bowman, 2002). Labelling experiments confirmed that BafA and ConmyA share the same binding site on subunit c (Huss *et al.*, 2002; Fernandes *et al.*, 2006). It has been suggested that these plecomacrolides prevent the rotation of the V_0 multimer which in turn blocks proton translocation (Bowman *et al.*, 2004). This subunit is critical for many v-ATPase functions and homozygous knockout mice do not survive beyond the embryonic stage (Futai *et al.*, 2000).

In contrast, SaliA and probably SaliPhe do not bind to subunit c directly (Huss *et al.*, 2005), but act on the transmembrane proton translocation domain (Lebreton *et al.*, 2008). The better antiviral effect/toxicity profile of SaliPhe over BafA *in vitro*, but in particular *in vivo*, may be due to the different binding sites of the two groups of compounds. However, the toxicity of BafA cannot be solely attributed to its v-ATPase inhibiting activity. It has been shown in BafA-resistant cells that exposure of up to 1 μM BafA did not induce cell death or inhibit cell growth despite its uncompromised effect on lysosomal pH (Tanigaki *et al.*, 2003). This indicates that v-ATPase inhibition and cytotoxicity of BafA rely on different mechanisms and can be pharmacologically dissociated. Thus, in the future, v-ATPase inhibitors with even better selective indices may become available for the treatment of viral infections.

The lower efficacy of v-ATPase inhibitors against H5N1 may suggest that this isolate may be less dependent on low endosomal pH. Certain mutations in the haemagglutinin of H5N1 (albeit not present in the H5N1 strain used in this study) have been recently described to render haemagglutinin activation less dependent on acidification required for viral entry (Reed *et al.*, 2010). However, these studies also showed that such mutations are not compatible with sustainable infections at least in mallards (Reed *et al.*, 2010).

Screening for host factors required for virus replication has been conducted for numerous viruses including HIV (König *et al.*, 2008), West Nile virus (Krishnan *et al.*, 2008), dengue (Sessions *et al.*, 2009) and influenza virus (Hao *et al.*, 2008; Brass *et al.*, 2009; König *et al.*, 2010; Karlas *et al.*, 2010). Interestingly, all of theses viruses require one or more v-ATPase subunits to establish infection (Table 1). Surprisingly, HIV-1 replication also requires a subunit of v-ATPase, although earlier studies indicated that viral entry was independent of endosomal acidification (Stein *et al.*, 1987), suggesting that other functions of v-ATPase could be involved (Peters *et al.*, 2001; Bayer *et al.*, 2003). Thus the v-ATPase may not only be a cellular target for the treatment of influenza but also of other viral infections that depend on this cellular protein.

In conclusion, our results show that the transmembrane proton translocating domain of cellular v-ATPase responsible for endosomal acidification can be selectively targeted by a new generation v-ATPase inhibitor with reduced toxicity to treat influenza virus infection including multi-resistant strains. Treatment strategies against influenza that target cellular proteins are expected to be more resistant to virus mutations than drugs blocking viral proteins.

Acknowledgements

The authors acknowledge the generous gift of ArchB from Prof Dr Dirk Trauner (Munich). We thank Gerard Grignard (Luxembourg) for the immunohistochemistry staining and Dominique Revets (Luxembourg) for preparing the microscopic images. We acknowledge Prof Dr Stephan Becker for providing A/Hamburg/01/2009 (S-OIV). We particularly acknowledge the support of F. Miguel L. Cardoso and Itati Ibanez (Ghent) for performing mouse experiments and the contribution of Andrej Egorov and Markus Wolschek (Vienna) in creating the PR8-NS116-GFP IAV virus. We thank Aurélie Sausy, Emilie Charpentier and Sébastien De Landt-

sheer (Luxembourg) for their excellent technical assistance. KHM is supported by a grant of Fonds National de la Recherche Luxembourg.

Conflicts of interest

The authors declare no conflict of interest.

References

Bayer MJ, Reese C, Buhler S, Peters C, Mayer A (2003). Vacuole membrane fusion: V0 functions after trans-SNARE pairing and is coupled to the Ca2+-releasing channel. J Cell Biol 162: 211–222.

Bowman BJ, Bowman EJ (2002). Mutations in subunit C of the vacuolar ATPase confer resistance to bafilomycin and identify a conserved antibiotic binding site. J Biol Chem 277: 3965–3972.

Bowman EJ, Graham LA, Stevens TH, Bowman BJ (2004). The bafilomycin/concanamycin binding site in subunit c of the V-ATPases from Neurospora crassa and Saccharomyces cerevisiae. J Biol Chem 279: 33131–33138.

Boyd MR, Farina C, Belfiore P, Gagliardi S, Kim JW, Hayakawa Y *et al.* (2001). Discovery of a novel antitumor benzolactone enamide class that selectively inhibits mammalian vacuolar-type (H+)-atpases. J Pharmacol Exp Ther 297: 114–120.

Brass AL, Huang IC, Benita Y, John SP, Krishnan MN, Feeley EM *et al.* (2009). The IFITM proteins mediate cellular resistance to influenza A H1N1 virus, West Nile virus, and dengue virus. Cell 139: 1243–1254.

De Jong MD, Tran TT, Truong HK, Vo MH, Smith GJ, Nguyen VC *et al.* (2005). Oseltamivir resistance during treatment of influenza A (H5N1) infection. N Engl J Med 353: 2667–2672.

Ducatez MF, Olinger CM, Owoade AA, Tarnagda Z, Tahita MC, Sow A *et al.* (2007). Molecular and antigenic evolution and geographical spread of H5N1 highly pathogenic avian influenza viruses in western Africa. J Gen Virol 88: 2297–2306.

Erickson KL, Beutler JA, Cardellina IJ, Boyd MR (1997). Salicylihalamides A and B, Novel Cytotoxic Macrolides from the Marine Sponge Haliclona sp. J Org Chem 62: 8188–8192.

Fernandes F, Loura LM, Fedorov A, Dixon N, Kee TP, Prieto M *et al.* (2006). Binding assays of inhibitors towards selected V-ATPase domains. Biochim Biophys Acta 1758: 1777–1786.

Forgac M (1999). Structure and properties of the vacuolar (H+)-ATPases. J Biol Chem 274: 12951–12954.

Futai M, Oka T, Sun-Wada G, Moriyama Y, Kanazawa H, Wada Y (2000). Luminal acidification of diverse organelles by V-ATPase in animal cells. J Exp Biol 203: 107–116.

Garcia-Sastre A, Egorov A, Matassov D, Brandt S, Levy DE, Durbin JE *et al.* (1998). Influenza A virus lacking the NS1 gene replicates in interferon-deficient systems. Virology 252: 324–330.

Gerloff NA, Kremer JR, Mossong J, Opp M, Muller CP (2009). Genomic diversity of oseltamivir-resistant influenza virus A (H1N1), Luxembourg, 2007–08. Emerg Infect Dis 15: 1523–1524.

Guinea R, Carrasco L (1995). Requirement for vacuolar proton-ATPase activity during entry of influenza virus into cells. J Virol 69: 2306–2312.

Hao L, Sakurai A, Watanabe T, Sorensen E, Nidom CA, Newton MA *et al.* (2008). Drosophila RNAi screen identifies host genes important for influenza virus replication. Nature 454: 890–893.

Hinton A, Bond S, Forgac M (2009). V-ATPase functions in normal and disease processes. Pflugers Arch 457: 589–598.

Huss M, Ingenhorst G, Konig S, Gassel M, Drose S, Zeeck A *et al.* (2002). Concanamycin A, the specific inhibitor of V-ATPases, binds to the V(o) subunit c. J Biol Chem 277: 40544–40548.

Huss M, Sasse F, Kunze B, Jansen R, Steinmetz H, Ingenhorst G *et al.* (2005). Archazolid and apicularen: novel specific V-ATPase inhibitors. BMC Biochem 6: 13.

Karlas A, Machuy N, Shin Y, Pleissner KP, Artarini A, Heuer D *et al.* (2010). Genome-wide RNAi screen identifies human host factors crucial for influenza virus replication. Nature 463: 818–822.

Kiso M, Mitamura K, Sakai-Tagawa Y, Shiraishi K, Kawakami C, Kimura K *et al.* (2004). Resistant influenza A viruses in children treated with oseltamivir: descriptive study. Lancet 364: 759–765.

Kittel C, Sereinig S, Ferko B, Stasakova J, Romanova J, Wolkerstorfer A *et al.* (2004). Rescue of influenza virus expressing GFP from the NS1 reading frame. Virology 324: 67–73.

König R, Zhou Y, Elleder D, Diamond TL, Bonamy GM, Irelan JT *et al.* (2008). Global analysis of host-pathogen interactions that regulate early-stage HIV-1 replication. Cell 135: 49–60.

König R, Stertz S, Zhou Y, Inoue A, Heinrich Hoffmann H, Bhattacharyya S *et al.* (2010). Human host factors required for influenza virus replication. Nature 463: 813–817.

Krishnan MN, Ng A, Sukumaran B, Gilfoy FD, Uchil PD, Sultana H *et al.* (2008). RNA interference screen for human genes associated with West Nile virus infection. Nature 455: 242–245.

Lackenby A, Hungnes O, Dudman SG, Meijer A, Paget WJ, Hay AJ *et al.* (2008). Emergence of resistance to oseltamivir among influenza A(H1N1) viruses in Europe. Euro Surveill 13: pii 8026.

Lebreton S, Jaunbergs J, Roth MG, Ferguson DA, De Brabander JK (2008). Evaluating the potential of vacuolar ATPase inhibitors as anticancer agents and multigram synthesis of the potent salicylihalamide analog saliphenylhalamide. Bioorg Med Chem Lett 18: 5879–5883.

Li YP, Chen W, Liang Y, Li E, Stashenko P (1999). Atp6i-deficient mice exhibit severe osteopetrosis due to loss of osteoclast-mediated extracellular acidification. Nat Genet 23: 447–451.

Mak GZ, Kavanaugh GM, Buschmann MM, Stickley SM, Koch M, Goss KH *et al.* (2006). Regulated synthesis and functions of laminin 5 in polarized Madin-Darby canine kidney epithelial cells. Mol Biol Cell 17: 3664–3677.

Mazur I, Wurzer WJ, Ehrhardt C, Pleschka S, Puthavathana P, Silberzahn T *et al.* (2007). Acetylsalicylic acid (ASA) blocks influenza virus propagation via its NF-kappaB-inhibiting activity. Cell Microbiol 9: 1683–1694.

Nishi T, Forgac M (2002). The vacuolar (H+)-ATPases–nature's most versatile proton pumps. Nat Rev Mol Cell Biol 3: 94–103.

Ochiai H, Sakai S, Hirabayashi T, Shimizu Y, Terasawa K (1995). Inhibitory effect of bafilomycin A1, a specific inhibitor of vacuolar-type proton pump, on the growth of influenza A and B viruses in MDCK cells. Antiviral Res 27: 425–430.

Ott S, Wunderli-Allenspach H (1994). Effect of the virostatic Norakin (triperiden) on influenza virus activities. Antiviral Res 24: 37–42.

Pastor-Soler N, Pietrement C, Breton S (2005). Role of acid/base transporters in the male reproductive tract and potential consequences of their malfunction. Physiology (Bethesda) 20: 417–428.

Perez L, Carrasco L (1994). Involvement of the vacuolar H(+)-ATPase in animal virus entry. J Gen Virol 75: 2595–2606.

Peters C, Bayer MJ, Buhler S, Andersen JS, Mann M, Mayer A (2001). Trans-complex formation by proteolipid channels in the terminal phase of membrane fusion. Nature 409: 581–588.

Reed LJ, Muench H (1938). A simple method for estimating fifty percent endpoints. Am J Hyg 27: 493–497.

Reed ML, Bridges OA, Seiler P, Kim JK, Yen HL, Salomon R *et al.* (2010). The pH of activation of the hemagglutinin protein regulates H5N1 influenza virus pathogenicity and transmissibility in ducks. J Virol 84: 1527–1535.

Sessions OM, Barrows NJ, Souza-Neto JA, Robinson TJ, Hershey CL, Rodgers MA *et al.* (2009). Discovery of insect and human dengue virus host factors. Nature 458: 1047–1050.

Shapira SD, Gat-Viks I, Shum BO, Dricot A, De Grace MM, Wu L *et al.* (2009). A physical and regulatory map of host-influenza interactions reveals pathways in H1N1 infection. Cell 139: 1255–1267.

Smith AN, Skaug J, Choate KA, Nayir A, Bakkaloglu A, Ozen S *et al.* (2000). Mutations in ATP6N1B, encoding a new kidney vacuolar proton pump 116-kD subunit, cause recessive distal renal tubular acidosis with preserved hearing. Nat Genet 26: 71–75.

Smith AN, Lovering RC, Futai M, Takeda J, Brown D, Karet FE (2003). Revised nomenclature for mammalian vacuolar-type H+ -ATPase subunit genes. Mol Cell 12: 801–803.

Stein BS, Gowda SD, Lifson JD, Penhallow RC, Bensch KG, Engleman EG (1987). pH-independent HIV entry into CD4-positive T cells via virus envelope fusion to the plasma membrane. Cell 49: 659–668.

Stephenson I, Democratis J, Lackenby A, Mcnally T, Smith J, Pareek M *et al.* (2009). Neuraminidase inhibitor resistance after oseltamivir treatment of acute influenza A and B in children. Clin Infect Dis 48: 389–396.

Sun-Wada GH, Yoshimizu T, Imai-Senga Y, Wada Y, Futai M (2003). Diversity of mouse proton-translocating ATPase: presence of multiple isoforms of the C, d and G subunits. Gene 302: 147–153.

Tanigaki K, Sasaki S, Ohkuma S (2003). In bafilomycin A1-resistant cells, bafilomycin A1 raised lysosomal pH and both prodigiosins and concanamycin A inhibited growth through apoptosis. FEBS Lett 537: 79–84.

Teplova VV, Tonshin AA, Grigoriev PA, Saris NE, Salkinoja-Salonen MS (2007). Bafilomycin A1 is a potassium ionophore that impairs mitochondrial functions. J Bioenerg Biomembr 39: 321–329.

Wang H, Wang Z, Wang S, Li M, Nan L, Rhie JK *et al.* (2005). Preclinical pharmacology of epothilone D, a novel tubulin-stabilizing antitumor agent. Cancer Chemother Pharmacol 56: 255–260.

Wang Y, Cipriano DJ, Forgac M (2007). Arrangement of subunits in the proteolipid ring of the V-ATPase. J Biol Chem 282: 34058–34065.

Ward CL, Dempsey MH, Ring CJ, Kempson RE, Zhang L, Gor D *et al.* (2004). Design and performance testing of quantitative real time PCR assays for influenza A and B viral load measurement. J Clin Virol 29: 179–188.

Xie XS, Padron D, Liao X, Wang J, Roth MG, De Brabander JK (2004). Salicylihalamide A inhibits the V0 sector of the V-ATPase through a mechanism distinct from bafilomycin A1. J Biol Chem 279: 19755–19763.